

# DEUTSCHES ELEKTRONEN-SYNCHROTRON

DESY 93-129  
September 1993



## Weak and Superweak Processes at HERA

W. Buchmüller

*Deutsches Elektronen-Synchrotron DESY, Hamburg*

ISSN 0418-9833

**NOTKESTRASSE 85 - 22603 HAMBURG**

DESY behält sich alle Rechte für den Fall der Schutzrechtserteilung und für die wirtschaftliche Verwertung der in diesem Bericht enthaltenen Informationen vor.

DESY reserves all rights for commercial use of information included in this report, especially in case of filing application for or grant of patents.

To be sure that your preprints are promptly included in the  
HIGH ENERGY PHYSICS INDEX,  
send them to (if possible by air mail):

**DESY  
Bibliothek  
Notkestraße 85  
22603 Hamburg  
Germany**

**DESY-IfH  
Bibliothek  
Platanenallee 6  
15738 Zeuthen  
Germany**

## 1 Introduction

At the electron-proton storage ring HERA inelastic scattering processes of electrons and protons can be studied at center-of-mass energies up to 314 GeV which, on the average, corresponds to a c.m.s energy of about 130 GeV in the electron-quark subsystem. The investigation of  $ep$ -scattering at HERA is complementary to the study of  $e^+e^-$ -annihilation at LEP and  $p\bar{p}$ -annihilation at the Tevatron.

Since the c.m.s. energy at HERA exceeds the masses of the intermediate vector bosons of the electroweak interactions, it is possible to perform novel tests of the electroweak theory in the electron-quark sector. As we shall see, the study of the charged current at large momentum transfer will be of particular interest. Production processes of W-bosons and Z-bosons will probe vector boson self-couplings, and they are also important as a source of events similar to those expected from new physics.

Physics beyond the standard model could be revealed through new short range interactions, induced by the exchange of new particles which are too heavy to be produced directly. The flavour structure and the strength of such contact interactions would then allow to draw conclusions on the dynamics and the mass scale of the new physics. Of course, one can also directly produce new heavy particles in electron-quark scattering. Depending on the quantum numbers, some particles are more effectively produced in  $ep$ -scattering than in  $e^+e^-$  or  $p\bar{p}$ -annihilation.

In the following chapters we shall discuss these topics in turn. We shall first describe the different electroweak processes, i.e., neutral and charged current inelastic scattering and the production of vector bosons. This will lead us to a discussion of electroweak precision tests, followed by a review of contact interactions. There is a variety of new particles which can be produced in high-energy electron-proton scattering. In some detail we shall consider the production of super-particles, leptoquarks and heavy neutrinos.

To a large extent these lectures are based on results obtained in two workshops on Physics at HERA which took place in recent years at DESY [1], [2]. Some complementary discussions can be found in [3] - [5].

## 2 Electroweak processes

The two main electroweak processes are inelastic neutral current (NC) and charged current (CC) scattering. Of interest are also the production of charged and neutral

# Weak and Superweak Processes at HERA \*

W. Buchmüller

*Deutsches Elektronen-Synchrotron DESY, 2000 Hamburg 52, Germany*

### Contents

1. Introduction
2. Electroweak processes
3. Electroweak precision tests
4. Contact interactions
5. New particles
6. Summary

\*Lectures given at the XXI International Meeting on Fundamental Physics, Miraflores de la Sierra, Madrid, May 1993

intermediate vector bosons, and radiative charged current scattering. All these processes test certain aspects of the electroweak theory, and we will discuss them one by one. From LEP we know that the standard model Higgs boson is heavier than about 60 GeV. The production cross section for Higgs bosons in this mass range in  $ep$ -scattering is too small to be of relevance at HERA [6].

## 2.1 Neutral current and charged current processes

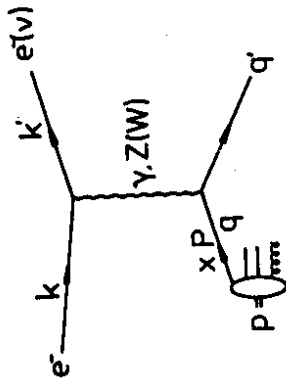


Figure 1. Inelastic electron-proton scattering

The inelastic scattering of left-handed and right-handed electrons off protons (cf. fig.(1)),

$$e_{L,R}(k) + p(P) \rightarrow e'_{L,R}(k') + X(P_X) \quad (1)$$

is described by the differential cross section

$$\begin{aligned} \frac{d^2\sigma^{NC}}{dx dy} (e_{L,R}P) &= x s \frac{d^2\sigma^{NC}}{dx dQ^2} (e_{L,R}P) \\ &= \frac{2\pi\alpha^2}{x^2 y^2 s} \left[ 2(1-y) F_2^{L,R}(x, Q^2) + 2xy^2 F_1^{L,R}(x, Q^2) \right. \\ &\quad \left. + (1-(1-y)^2) x F_3^{L,R}(x, Q^2) \right]. \end{aligned} \quad (2)$$

Here  $s$ ,  $Q^2$ ,  $x$  and  $y$  are the usual kinematic variables<sup>1</sup>

$$s = (k + P)^2, \quad Q^2 = -(k - k')^2, \quad x = \frac{Q^2}{2P \cdot (k - k')}, \quad y = \frac{P \cdot (k - k')}{P \cdot k}, \quad (3)$$

<sup>1</sup>We follow the notation of [7]

which, neglecting masses, satisfy the relation

$$Q^2 = x y s \quad (4)$$

In eq. (2) we have neglected the proton mass compared to the c.m.s. energy  $s$ , which at HERA is 314 GeV. At large values of  $x$  and  $Q^2$ , which are relevant for tests of the electroweak theory, the Callan-Gross relation

$$F_2^{L,R} = 2 x F_1^{L,R} \quad (5)$$

holds to good approximation. QCD corrections, which violate this relation, are negligible, and the number of independent structure functions in eq. (2) is reduced from three to two. Note, however, that the Callan-Gross relation does not necessarily hold for spin- $\frac{1}{2}$  partons. As we shall discuss in sect. 4, chirality changing interactions could lead to observable deviations.

In the quark-parton model the structure functions are obtained by summing incoherently over all elastic electron-quark and electron-antiquark scattering processes. In this way the structure functions are related to the parton densities in the proton:

$$F_2^{L,R} = \sum_q x (f_q(x, Q^2) + f_{\bar{q}}(x, Q^2)) (|V_q^{L,R}(Q^2)|^2 + |A_q^{L,R}(Q^2)|^2), \quad (6)$$

$$F_3^{L,R} = \pm \sum_q x (f_q(x, Q^2) - f_{\bar{q}}(x, Q^2)) V_q^{L,R}(Q^2) A_q^{L,R}(Q^2), \quad (7)$$

where  $f_q$  and  $f_{\bar{q}}$  denote the quark and anti-quark densities, respectively. The electroweak form factors  $V_q^{L,R}(Q^2)$  and  $A_q^{L,R}(Q^2)$  depend on the electric charges ( $Q_e, Q_q$ ) and the vector ( $v_e, v_q$ ) and axial-vector ( $a_e, a_q$ ) couplings of electron and quarks to the Z-boson:

$$V_q^{L,R}(Q^2) = Q_e Q_q + (v_e \pm a_e) v_q \frac{Q^2}{Q^2 + m_Z^2}, \quad (8)$$

$$A_q^{L,R}(Q^2) = -(v_e \pm a_e) a_q \frac{Q^2}{Q^2 + m_Z^2}. \quad (9)$$

These form factors arise from the interference between photon and Z-boson exchange.

In the standard model of electroweak interactions vector and axial-vector couplings of electron and quarks can be expressed in terms of electric charge, weak isospin ( $T_3$ ) and the weak angle  $\theta_W$ , or, equivalently, in terms of the Fermi constant  $G_F$ , the Z-boson mass  $m_Z$  and the fine-structure constant  $\alpha$  ( $f = e, q$ ):

$$v_f = \frac{1}{\sin 2\theta_W} (T_3^f - 2Q_f \sin^2 \theta_W), \quad a_f = \frac{1}{\sin 2\theta_W} T_3^f, \quad (10)$$

where

$$\sin^2 \theta_W = 1 - \frac{m_W^2}{m_Z^2}, \quad \frac{1}{\sin 2\theta_W} = \frac{1}{2} \left( \frac{\sqrt{2} G_\mu m_Z^2}{\pi \alpha} \right)^{1/2} \quad (11)$$

The relation between the weak angle and the vector boson masses holds at tree-level. If radiative corrections are included this is one possible definition of the weak angle.

In addition to inelastic electron-proton scattering inelastic positron-proton scattering is of interest,

$$e_{L,R}^+ p \rightarrow e_{L,R}^+ X \quad (12)$$

The corresponding differential cross section can easily be obtained from eq. (2). For charge conjugated spinors  $\psi^c = C\bar{\psi}^T$  one has the relation  $\bar{\psi}^c \gamma^\mu \psi^c = -\bar{\psi} \gamma^\mu \psi$  ( $v \rightarrow -v$ ) and  $\psi^c \gamma^\mu \psi^c = \bar{\psi} \gamma^\mu \psi$  ( $v \rightarrow v$ ). Thus the substitution  $e^- \rightarrow e^+$  corresponds to the substitutions  $(Q_e, v_e, a_e) \rightarrow (-Q_e, -v_e, a_e)$ . This implies for the structure functions

$$F_2^{L,R} \rightarrow F_2^{R,L}, \quad F_3^{L,R} \rightarrow -F_3^{R,L} \quad (13)$$

In addition to neutral current processes charged current reactions are of importance at HERA. The standard model predicts the differential cross section

$$\begin{aligned} \frac{d^2 \sigma^{CC}}{dx dy} (e_{L,R}^- p) &= x s \frac{d^2 \sigma^{CC}}{dx dy} (e_{L,R}^- p) \\ &= \frac{G_\mu^2 s}{4\pi (Q^2 + m_W^2)^2} \left[ 2(1-y) F_2^{CC}(x, Q^2) + 2xy^2 F_1^{CC}(x, Q^2) \right. \\ &\quad \left. + (1 - (1-y)^2) x F_3^{CC}(x, Q^2) \right]. \end{aligned} \quad (14)$$

The structure of the differential cross is very similar to the neutral current cross section, yet the relation between structure functions and parton densities is different,

$$F_2^{CC}(x, Q^2) = \sum_{i=1}^3 x (f_u(x, Q^2) + f_d(x, Q^2)), \quad (15)$$

$$F_3^{CC}(x, Q^2) = \sum_{i=1}^3 (f_u(x, Q^2) - f_d(x, Q^2)), \quad (16)$$

where the sum extends over the three families.

The differential cross section for inelastic positron proton scattering,

$$e^+ p \rightarrow \bar{\nu}_e X, \quad (17)$$

can again be obtained from eq. (14) by the substitution

$$F_{1,2}^{CC} \rightarrow F_{1,2}^{CC}, \quad F_3^{CC} \rightarrow -F_3^{CC} \quad (18)$$

Since the charged current interaction is purely left-handed in the standard model several noteworthy relations hold:

$$\frac{d^2 \sigma^{CC}}{dx dy} (e^- p) = \frac{1}{2} \frac{d^2 \sigma^{CC}}{dx dy} (e_L^- p), \quad (19)$$

$$\frac{d^2 \sigma^{CC}}{dx dy} (e^- p) = \frac{d^2 \sigma^{CC}}{dx dy} (e_L^- p) = 0. \quad (20)$$

The order of magnitude of the total charged current cross section is  $\sigma_{tot}^{CC} \sim G_F^2 s / 4\pi \sim 100 \text{ pb}$  at the HERA c.m.s. energy. Hence, one year of running at the design luminosity of  $\sim 100 \text{ pb}^{-1}$  is expected to yield about  $10^4$  charged current events.

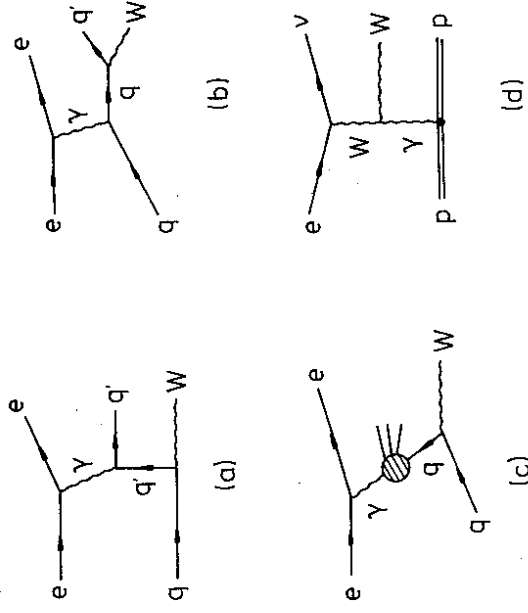


Figure 2. Some production processes for W-bosons

## 2.2 Production of vector bosons

In inelastic electron-proton collisions photons, W-bosons and Z-bosons can be produced. Some of the subprocesses which contribute to the production of W-bosons are shown in fig. (2). A complete list of the different production processes is

$$\begin{aligned} e^- p &\rightarrow e^- \gamma X, \\ e^- p &\rightarrow \nu \gamma X, \end{aligned}$$

In recent years more elaborate detailed calculations for vector boson production in  $e\bar{p}$ -collisions have been carried out [9]. In addition to the direct photon contribution discussed above the resolved photon contribution (cf. fig. (2c)) has been taken into account which turns out to be indeed non-negligible. In the case of  $Z$ -boson production both contributions are about equal. Furthermore, the intriguing clean diffractive processes (cf. fig. (2d))

$$\begin{aligned} e^- p &\rightarrow \nu W^- p, \\ e^- p &\rightarrow e^- Z p, \end{aligned} \quad (27)$$

have been studied. In table (2.2) we have listed the results of the detailed investigation of Baur, Vermaseren and Zeppenfeld. The total production cross section of  $W$ -bosons turns out to be about 1 pb.

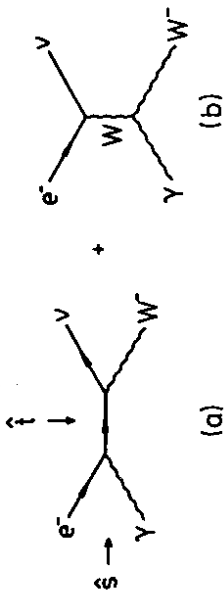


Figure 3. Subprocesses for  $e^- p \rightarrow \nu W^- X$ .

The precise knowledge of the production cross sections for vector bosons is important since their decays into final states with neutrinos lead to events with a large amount of missing energy which are an important background for signals of new physics beyond the standard model.

### 2.3 Anomalous $WW\gamma$ couplings

The production of vector bosons at HERA can be used to test the standard model predictions for the couplings of  $W$ -bosons to photons. In extensions of the standard model the effective lagrangian for the interactions of photons and  $W$ -bosons has to be invariant only under the  $U(1)$  symmetry of electromagnetism. One then has (cf. [10]):

$$\mathcal{L} = -ie(W_{\mu\nu}^\dagger W^{\mu\nu} A^\nu - W_{\mu\nu} W^{\mu\nu} A^\nu + \kappa W_\mu^\dagger W_\nu F^{\mu\nu} + \frac{\lambda}{m_W^2} W_{\mu\nu}^\dagger W_\sigma F^{\sigma\mu} + \dots), \quad (28)$$

$$\begin{aligned} e^- p &\rightarrow e^- W^+ X, \\ e^- p &\rightarrow \nu W^- X, \\ e^- p &\rightarrow e^- Z X, \\ e^- p &\rightarrow \nu Z X. \end{aligned} \quad (21)$$

To good approximation the corresponding cross sections can be evaluated in the Weizsäcker-Williams approximation, where the on-shell photon may be emitted either from the electron or one of the quarks and anti-quarks inside the proton. As an example consider the process  $e^- p \rightarrow \nu W^- X$ , for which the subprocesses are shown in fig. (3). The related cross section reads (cf. [8]):

$$\hat{\sigma}(s, \hat{s}, \hat{t}, \hat{u}) = \frac{\pi\alpha^2}{\sin^2\theta_W} \left( \frac{2m_W^2 - t}{\hat{s}} + \frac{2(\hat{t} - m_W^2 - m_W^4/\hat{s})}{\hat{s} + \hat{t}} + \frac{2m_W^4 - 2\hat{s}\hat{t}}{(\hat{s} + \hat{t})^2} \right). \quad (22)$$

Here  $\hat{s}$ ,  $\hat{t}$  and  $\hat{u}$  are the usual Mandelstam variables of the parton subprocesses (cf. fig. (3)). The flux of photons from the proton is obtained by summing the Weizsäcker-Williams densities for all quarks:

$$P_{\gamma|p}(x) = \int_0^1 dx_1 \sum_q (f_q(x_1, Q_{WW}^2) + f_{\bar{q}}(x_1, Q_{WW}^2)) \int_0^1 dx_2 P_{\gamma|q}(x_2) \delta(x - x_1 x_2), \quad (23)$$

where the Weizsäcker-Williams spectrum reads

$$P_{\gamma|q}(x) = \frac{\alpha}{2\pi} Q_q^2 \frac{1 + (1-x)^2}{x} \ln \frac{Q_{max}^2}{Q_{min}^2}, \quad (24)$$

and the maximal momentum transfer is

$$Q_{max}^2 = xs - m_W^2. \quad (25)$$

For the minimal momentum transfer one chooses typically  $Q_{min} = 1 \text{ GeV}$ . In eq. (23) the mass scale  $Q_{WW}^2$  has to be suitably defined [8].

The total production cross section for  $W$ -bosons is now given by

$$\sigma_{\nu W^-} = \int_{m_W^2/s}^1 dx P_{\gamma|p}(x) \hat{\sigma}(s, \hat{s}, \hat{t}, \hat{u}). \quad (26)$$

The cross section is rather small, about 0.1 pb. The order of magnitude is easily understood. Compared to the charged current cross section  $\sigma^{CC} \sim 100 \text{ pb}$ , there is one more power of  $\alpha$ . Furthermore, the additional particle in the final state leads to a phase space suppression factor. One estimates  $\sigma_{\nu W} \sim (\alpha/2\pi)\sigma^{CC}$ , which yields about 1 pb.

process	$\sigma(pb)$
$ep \rightarrow eW^+X$	0.50 - 0.72
$ep \rightarrow eW^-X$	0.47 - 0.62
$ep \rightarrow \nu W^-X$	0.064
$ep \rightarrow eZX$	0.34 - 0.43
$ep \rightarrow \nu ZX$	0.0044
$ep \rightarrow W^+X$	0.50 - 0.72
$ep \rightarrow W^-X$	0.53 - 0.68
$ep \rightarrow ZX$	0.34 - 0.43
$ep \rightarrow \nu W^-p$	0.026
$ep \rightarrow eZp$	0.117

Table 1: Total cross sections for the production of vector bosons in several processes. From [9].

where  $W_{\mu\nu} = \partial_\mu W_\nu - \partial_\nu W_\mu$  and  $F_{\mu\nu} = \partial_\mu A_\nu - \partial_\nu A_\mu$  are the usual field strength tensors. The parameters  $\kappa$  and  $\lambda$  are related to the magnetic dipole moment and the electric quadrupole moment of the W-boson:

$$\mu_W = \frac{e}{2M_W}(1 + \kappa + \lambda), \quad (29)$$

$$Q_W = -\frac{e}{M_W^2}(\kappa - \lambda). \quad (30)$$

In the standard model one has

$$\kappa - 1 = 0, \quad \lambda = 0. \quad (31)$$

The most general effective lagrangian (28) contains further parity and C-parity breaking terms which, however, cannot be probed at HERA.

The cross sections for the production of vector bosons are sensitive to the anomalous couplings  $\kappa - 1$  and  $\lambda$ . Based on the leptonic decays  $W^\pm \rightarrow e^\pm \nu$ ,  $\mu^\pm \nu$  and an integrated luminosity of  $1000 \text{ pb}^{-1}$  Baur and Zeppenfeld [11] estimate for the  $1\sigma$  errors of the anomalous couplings, which can be obtained at HERA,

$$\kappa - 1 \simeq \pm 0.36 \text{ (0.52)}; \quad \lambda \simeq \pm 0.88 \text{ (0.89)}. \quad (32)$$

Here an uncertainty of the standard model production cross section due to unknown QCD corrections of 10% (30%) has been assumed. The resolved photon contribution has not been taken into account explicitly.

Alternatively, one can consider charged current radiative events [12]-[14],

$$ep \rightarrow \nu \gamma X, \quad (33)$$

where the anomalous couplings lead to an enhancement of isolated photons with large transverse, unbalanced momentum. For an integrated luminosity of  $1000 \text{ pb}^{-1}$  Helbig and Spiesberger [12] find a sensitivity which corresponds to the  $1\sigma$  errors

$$\kappa - 1 \simeq \pm 1.0, \quad \lambda \simeq \pm 1.2. \quad (34)$$

Hence, the sensitivity to anomalous couplings seems to be smaller in radiative charged current scattering than in vector boson production. On the other hand, the radiative charged current events are free from the possibly large unknown QCD corrections present in vector boson production. In general, the limits on anomalous gauge couplings obtainable at HERA appear to be weaker than the bounds which can be expected from the Tevatron and LEP II within the next few years [14].

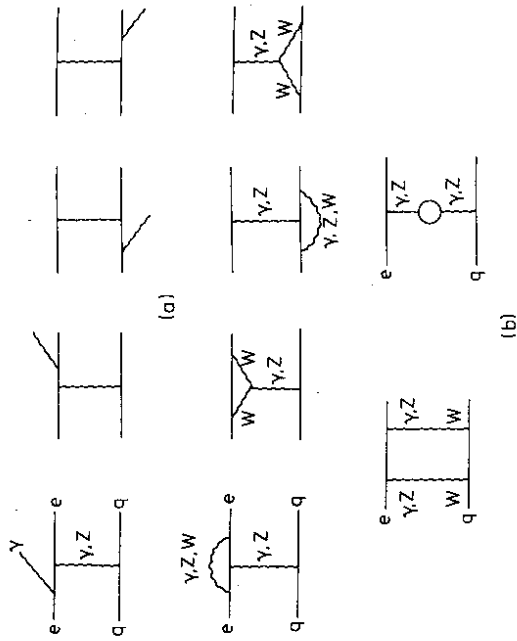


Figure 4. One-loop electroweak radiative corrections to neutral current scattering

### 3 Electroweak precision tests

Higher order electroweak corrections to neutral current scattering involves electromagnetic bremsstrahlung and electroweak virtual corrections (fig. (4)). A complete evaluation of the one-loop corrections has been performed independently by two groups [15]-[17]. The bremsstrahlung contribution has to be integrated over the region of phase space where the additional photon cannot be observed. This yields particularly large corrections at small values of  $x$  and  $Q^2$ . However, for electroweak precision tests the region  $Q^2 > 10^3 \text{ GeV}^2$  is important, and here the bremsstrahlung contribution is rather small.

In order to discuss next-to-leading order electroweak corrections one has to specify first of all a renormalization scheme. Convenient and transparent with respect to its physical meaning is the on-shell scheme where the electromagnetic fine-structure constant  $\alpha$  and the masses of W-boson ( $m_W$ ), Z-boson ( $m_Z$ ), Higgs-boson ( $m_H$ ) and top-quark ( $m_t$ ) appear as independent parameters. The Fermi constant, as measured in  $\mu$ -decay, is then a dependent quantity,

$$G_\mu = G_\mu(\alpha, m_W, m_Z, m_H, m_t) \quad (35)$$

Since the Fermi-constant is known to high precision it is often convenient to use instead a modified on-shell scheme where  $G_\mu$  replaces  $m_W$  as independent variable. One then has

$$m_W = m_W(\alpha, G_\mu, m_Z, m_H, m_t) \quad (36)$$

Since the dependence on  $m_H$  is rather weak, the present knowledge of vector boson masses and gauge couplings provides interesting upper and lower bounds on the mass of the top-quark.

The sum of the Born-amplitude and the one-loop corrections shown in fig. (4) can be expressed as sum of a dressed photon exchange amplitude and a dressed Z-boson exchange amplitude. The structure of the dressed amplitudes [18] is similar to the Born amplitudes, the main difference is the appearance of a variety of form factors. From eqs. (8-11) it is clear that the strength of the Z-exchange amplitudes are proportional to  $G_\mu m_Z^2$ . The one-loop corrections lead to a formfactor [18]

$$G_\mu m_Z^2 \rightarrow G_\mu m_Z^2 \rho_{eq}(x, Q^2) \quad (37)$$

where

$$\rho_{eq}(x, Q^2) = 1 + \Delta\rho + \Delta_{eq}(x, Q^2) \quad (38)$$

Here

$$\Delta = \frac{3\alpha}{4\pi} \frac{m_t^2}{\sin^2 2\theta_W m_Z^2} \quad (39)$$

is a universal part and  $\Delta_{eq}$  an additional non-universal correction. Similarly, the mixing angle which appears in the vector coupling  $v_f$  (cf. (10)) now becomes a form factor which depends on the quark species [18]

$$\sin \theta_W \rightarrow s_{eq}(x, Q^2) \quad (40)$$

where

$$s_{eq}^2(x, Q^2) = \sin^2 \theta_W (1 + \cot^2 \theta_W \Delta\rho + \Delta_{eq}(x, Q^2)) \quad (41)$$

$\Delta_{eq}$  is again a nonuniversal contribution. In addition to the formfactors which affect normalization and  $Z - \gamma$  - mixing there are also some nonfactorizable terms [18]. The magnitude of the one-loop corrections to the Born amplitudes is of order 1%. The  $Q^2$ -dependence of some formfactors  $\rho_{eq}$  and  $s_{eq}$  is shown in figs. (5,6).

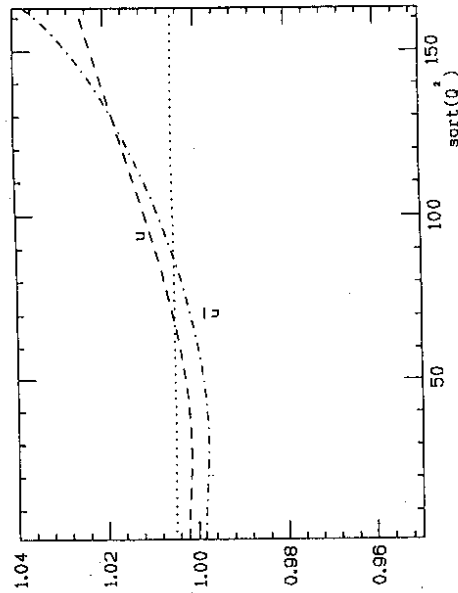


Figure 5. The NC form factor  $\rho_{eq}(x)$  for  $m_t = 130 \text{ GeV}$ . The horizontal dotted line corresponds to  $1 + \Delta\rho$ ,  $x = 0.3$ . From [18].



measurement restricts the  $W$ -mass with an error of

$$\delta m_W = \pm 160 \text{ MeV} \quad (43)$$

It is a non-trivial test of the electroweak theory that the "Fermi constants" at small and large values of  $Q^2$  yield consistent values of  $m_W$ . A further crucial test of the standard model, and a restriction on physics beyond the standard model, is the consistency between the  $W$ -boson masses determined from the propagator and from  $W$ -pair production at LEP II.

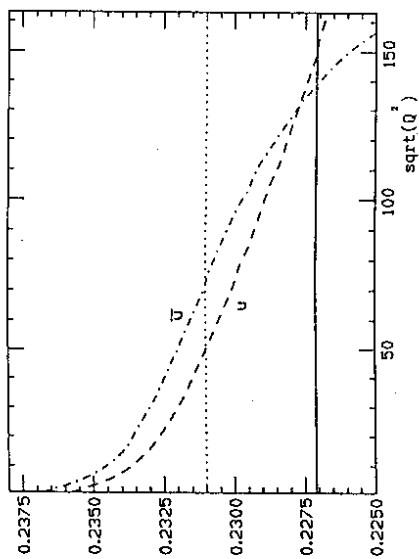


Figure 6. The effective mixing angle  $s^2_{\text{eff}}(q)$  for  $m_t = 130 \text{ GeV}$ . The horizontal full line denotes  $\sin^2 \theta_W$ , the dotted line corresponds to  $\sin^2 \theta_W (1 + \cot \theta_W) \Delta \rho$ ,  $x = 0.3$ . From [18].

What can we learn from precision measurements at HERA for the theory of electroweak interactions? A particularly useful quantity is the ratio

$$R_- = \frac{d\sigma^{NC}(x, Q^2)}{d\sigma^{CC}(x, Q^2)}, \quad (42)$$

integrated over some optimized range in  $x$  and  $Q^2$ . According to the analysis of Brisson et al. [19] a measurement of  $R_-$  with 1% accuracy appears ultimately feasible at HERA. For each Higgs mass this measurement defines a thin band in the  $m_W$ - $m_t$ -plane. For two Higgs masses these bands are shown in fig. (7). Also shown are the corresponding lines which result from the  $G_\mu$  constraint. There is a difference in curvature due to the propagator effect. Clearly, the measurement of  $R_-$  is effectively a determination of the Fermi "constant" at large values of  $Q^2$ , whereas muon decay yields a determination at  $Q^2 = 0$ . Both measurements restrict the  $W$ -boson mass with comparable accuracy. For instance, let us assume that the top-quark mass is known with an error of 10 GeV and that the central value is 130 GeV (a result with such an accuracy may eventually be obtained by the Tevatron experiments). One then reads off from fig. (7) that the  $R_-$

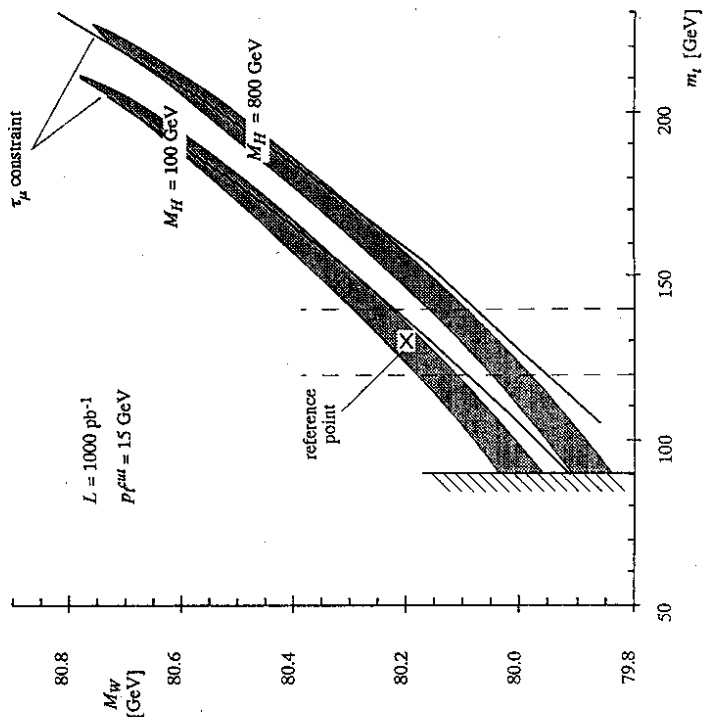


Figure 7.  $1\sigma$ -contours obtained from a measurement of  $R_-$  for two values of the Higgs mass. The two lines are the corresponding constraints from the muon lifetime. From [19].

## 4 Contact interactions

Low energy effects of new interactions with a mass scale  $\Lambda$  larger than the Fermi scale of weak interactions,  $\Lambda > 1/\sqrt{GF}$ , can be systematically studied by means of an effective, non-renormalizable lagrangian of the form

$$\mathcal{L}_{eff} = \mathcal{L}_0 + \frac{1}{\Lambda} \mathcal{L}_1 + \frac{1}{\Lambda^2} \mathcal{L}_2 + \dots \quad (44)$$

Here  $\mathcal{L}_0$  is the standard model lagrangian, and  $\mathcal{L}_1$  consists of the single term

$$\mathcal{L}_1 = \epsilon_{ij} \bar{\nu}_R^i \phi^j \epsilon_{kl} \bar{\nu}_R^k \phi^l + c.c. \quad (45)$$

which, after spontaneous symmetry breaking, gives rise to Majorana neutrino masses. Out of the many dimension-6 operators contained in  $\mathcal{L}_2$  the following contribute to lepton-nucleon scattering (cf., e.g. [20]):

$$\mathcal{L}_{contact}^{LN} = \mathcal{L}_V + \mathcal{L}_S + c.c., \quad (46)$$

$$\begin{aligned} \mathcal{L}_V = & \frac{(1)q}{\eta_{LL}^1} (\bar{\ell} \gamma_\mu \tau^\ell) (\bar{q} \gamma^\mu \tau^q) + \frac{(3)q}{\eta_{LL}^3} (\bar{\ell} \gamma_\mu \ell) (\bar{q} \gamma^\mu q) \\ & + \eta_{LR}^0 (\bar{\ell} \gamma_\mu \ell) (\bar{u} \gamma^\mu u) + \eta_{LR}^d (\bar{\ell} \gamma_\mu \ell) (\bar{d} \gamma^\mu d) \\ & + \eta_{RL}^0 (\bar{e} \gamma_\mu e) (\bar{q} \gamma^\mu q) \end{aligned} \quad (47)$$

$$\mathcal{L}_S = \eta_d (\bar{e} e) (\bar{d} q) + \eta_u (\bar{\ell} e) (\bar{q} u) + \tilde{\eta}_u (\bar{\ell} u) (\bar{q} e). \quad (48)$$

The  $SU(2)$ -doublets  $\ell = (\nu, e)$  and  $q = (u, d)$  denote left-handed fields ( $Ll = \ell, Lq = q, L = \frac{1-\gamma_5}{2}$ ) and the  $SU(2)$ -singlets  $e, u$  and  $d$  represent right-handed electron, up-quark and down-quark ( $Re = e, Ru = u, Rd = d, R = \frac{1+\gamma_5}{2}$ ). Possible tensor contact terms in the effective lagrangian (46) can be obtained by Fierz transformations from the terms already present.

From eq. (46) one obtains the effective lagrangian for neutral current processes [21],[22]:

$$\mathcal{L}_{contact}^{eN} = \mathcal{L}_V^e + \mathcal{L}_S^e \quad (49)$$

$$\begin{aligned} \mathcal{L}_V^e = & \sum_{q=u,d} [\eta_{LL}^e (\bar{e} \gamma_\mu e) (\bar{q} \gamma^\mu q_L) + \eta_{LR}^e (\bar{e} \gamma_\mu e) (\bar{q} \gamma^\mu q_R)] \\ & + \eta_{RL}^e (\bar{e} \gamma_\mu e) (\bar{q} \gamma^\mu q_L) + \eta_{RR}^e (\bar{e} \gamma_\mu e) (\bar{q} \gamma^\mu q_R), \end{aligned} \quad (50)$$

$$\mathcal{L}_S^e = \eta_d (\bar{e} \gamma_\mu e) (\bar{d} d_L) + \eta_u (\bar{e} \gamma_\mu e) (\bar{u} u_R) + \tilde{\eta}_u (\bar{e} \gamma_\mu e) (\bar{u} u_R). \quad (51)$$

Note, that due to the underlying  $SU(2) \times U(1)$  symmetry only three of the possible six helicity flip terms appear. Furthermore, among the helicity conserving contact terms one

has the relation

$$\eta_{RL}^e = \eta_{RL}^d \quad (52)$$

All other terms are independent. Of course, many relations between neutral and charged current contact terms can be read off from eq. (46). However, in the following we shall mainly consider neutral current contact terms which have been most extensively studied [23].

Contact interactions are generated by the exchange of heavy intermediate particles. Examples are leptons (c.f. sect. 5.2) such as  $S_0$  (with  $\lambda_L \neq 0$ ) or  $\tilde{S}_{1/2}$ . Both leptons induce only one non-vanishing coefficient  $\eta$ , respectively [23],

$$S_0 : \eta_{LL}^e = -\frac{1}{2} \frac{\lambda_L^2}{m_S^2}, \quad (53)$$

$$\tilde{S}_{1/2} : \eta_{LR}^d = -\frac{1}{2} \frac{\lambda_L^2}{m_{\tilde{S}}^2}. \quad (54)$$

For comparison, for the heavy neutral  $Z'$ -vector boson in left-right symmetric models one obtains very different non-vanishing  $\eta$ -coefficients:

$$\eta_{LL}^e = \eta_{LL}^d = \frac{g^2}{12\rho m_{Z'}^2}, \quad (55)$$

$$\eta_{RL}^e = \eta_{RL}^d = \frac{g^2(1-\rho)}{12\rho m_{Z'}^2}, \quad (56)$$

$$\eta_{LR}^e = \frac{g^2(1-3\rho)}{12\rho m_{Z'}^2}, \quad \eta_{LR}^d = \frac{g^2(1+3\rho)}{12\rho m_{Z'}^2}, \quad (57)$$

$$\eta_{RR}^e = \frac{\eta_{RL}^e \eta_{LR}^e}{\eta_{LL}^e}, \quad \eta_{RR}^d = \frac{\eta_{RL}^d \eta_{LR}^d}{\eta_{LL}^d}, \quad (58)$$

$$(59)$$

where

$$\rho = \frac{\cos 2\theta_W}{\sin^2 \theta_W}. \quad (60)$$

These examples illustrate that it is very important to disentangle the various different contact terms in order to identify the underlying physics.

The effect of contact terms on the neutral current cross sections for left-handed and right-handed electrons is easily evaluated. The result can be expressed as a change of the functions  $V_q^{L,R}(Q^2)$  and  $A_q^{L,R}(Q^2)$  defined in sect. (2.1). One finds (cf. [23]):

$$\Delta V_q^L(Q^2) = \frac{Q^2}{2\alpha} (\eta_{LL}^e + \eta_{LR}^e), \quad \Delta V_q^R(Q^2) = \frac{Q^2}{2\alpha} (\eta_{RL}^e + \eta_{RR}^e), \quad (61)$$

$$\Delta A_q^L(Q^2) = \frac{Q^2}{2\alpha} (\eta_{LL}^e - \eta_{LR}^e), \quad \Delta A_q^R(Q^2) = \frac{Q^2}{2\alpha} (\eta_{RL}^e - \eta_{RR}^e). \quad (62)$$

	$e_L^-$	$e_R^-$	$e_L^+ + e_R^+$	$e_L^+$	$e_R^+$	$e_L^- + e_R^-$	$e_L^+ + e_R^+$
$S_0(\lambda_L)$	1.28	0.43	0.99	0.30	0.92	0.71	
$S_0(\lambda_R)$	0.33	1.28	0.89	0.93	0.24	0.65	
$\tilde{S}_{1/2}$	0.48	0.22	0.38	0.29	0.62	0.51	
$Z'(\text{LR})$	0.25	0.61	0.41	0.42	0.42	0.18	

Table 2:  $2\sigma$  lower bounds on  $m_X/\lambda_X$  in  $\text{TeV}$ , based on  $100 \text{ pb}^{-1}$ . From [23].

An observed deviation from the standard model prediction for the neutral current cross section can now be related to a size of any single  $\eta$ -coefficient which is assumed to be non-zero. Recently, a detailed combined analysis for all 8  $\eta$ -parameters of the chirality conserving contact terms has been performed [23]. The sensitivity depends on the integrated luminosity and on the polarization of the incident electron or positron. For the examples described above the achievable lower bounds on  $m_X/\lambda_X$  are listed in table (4). In the general analysis one considers the 28 projections in the 8-dimensional  $\eta$ -space (cf. fig. (8)). The same technique has also been used to study systematically the effect of exchanged  $Z'$ -bosons [24].

From table (4) it is clear that the study of contact interactions is not very relevant for weakly coupled new particles. In this case the obtained mass bounds are so low that the particle under consideration can usually be directly produced. Interesting mass bounds are obtained for strongly coupled particles. For instance, for the leptoquark  $S_0$  with  $\lambda_L = \sqrt{4\pi}$  one obtains the mass bound  $m_S \approx 3.5 \text{ TeV}$ . In other cases, and also for the chirality changing contact terms, one can reach the mass scale ( $\eta \equiv 4\pi/\Lambda^2$ )

$$\Lambda \approx 7 \text{ TeV} \quad (63)$$

Even more stringent bounds can be obtained from a combination of neutral and charged current contact terms, which are related by  $SU(2)$ -invariance. In the case of the leptoquark  $S_0$  Doncheski and Hewett found the large mass scale [25]

$$\Lambda \approx 13 \text{ TeV} \quad (64)$$

The advantage of a contact term analysis is its model independence. As the above discussion shows a combined analysis of all contact terms, including charged current ones, can yield rather stringent bounds.

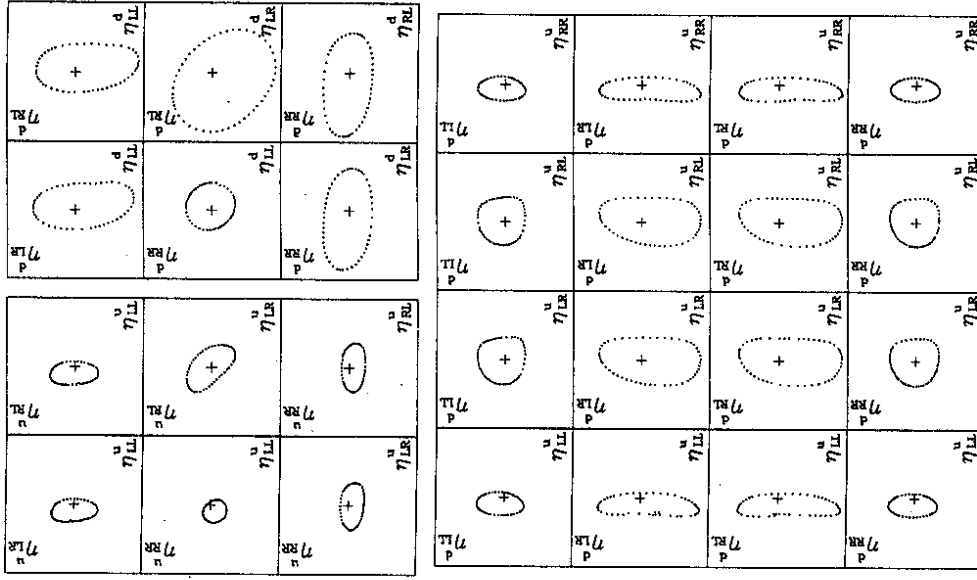


Figure 8. The 28 projections in the 8-dimensional  $\eta$ -space. Each side of the boxes ranges from  $-25$  to  $+25 \text{ TeV}^{-2}$ , the cross represents the standard model prediction. From [23].

## 5 New particles

The structure of the standard model of strong and electroweak interactions gives rise to a number of questions which lead us beyond the standard model:

- Do elementary scalar particles exist? This question applies first of all to the Higgs boson which is a crucial ingredient of the standard model. Unfortunately, the cross section for the electroweak production of Higgs bosons with masses above 60 GeV, the present mass limit from LEP, is too small to be measured at HERA. However, other scalar particles may exist which could be produced at HERA. All theories with quark-lepton unification predict leptoquarks with couplings to quark-lepton pairs. In some unified theories, especially those motivated by superstring theories, such leptoquarks are expected to have masses accessible at present and future accelerators.
- Is lepton number related to an exact or an approximate symmetry? Theoretically most appealing is the idea that lepton number is a spontaneously broken local symmetry. This is the case in extended gauge theories based on symmetry groups such as  $SU(3)_C \times SU(2)_L \times U(1)_Y \times U(1)_{X'}$  or  $SU(3)_C \times SU(2)_L \times SU(2)_R \times U(1)_{B-L}$ . These theories predict neutrino masses and also the existence of additional, very heavy neutrinos. If the mass scale of  $B - L$  - breaking is in the TeV range, one expects heavy neutrinos with masses between a few tens and a few hundred GeV.
- Are the mass scales of electroweak symmetry breaking and supersymmetry breaking the same? In this case we can look forward to whole zoo of new particles which should be discovered in the not to distant future. An intriguing hint in this direction is the non-trivial unification of gauge couplings [26] in the supersymmetric standard model which, however, could also just be a misleading numerical accident.

### 5.1 Supersymmetry

Let us first discuss the prospects for producing super-particles at HERA. In the supersymmetric standard model the particle content is roughly doubled. We have a set of matter and gauge fields  $\{\Phi_{i,\alpha}\}$  where the index  $i$  labels the species within the standard model, i.e., quarks, leptons, gauge bosons and Higgs particles.  $\alpha = 2$  then corresponds to all super-partners. Due to supersymmetry no new couplings are introduced whereas the mass spectrum of the super-particles is largely arbitrary.

Recently, several calculations of super-particle masses have been performed where the unification of the gauge couplings, the idea of radiative electroweak symmetry breaking and some constraints concerning fine-tuning of parameters have been implemented [27]. In a large class of models the masses of photino ( $\tilde{\gamma}$ ), zino ( $\tilde{z}$ ), winos ( $\tilde{w}$ ), scalar leptons ( $\tilde{l}$ ), scalar quarks ( $\tilde{q}$ ) and gluino ( $\tilde{g}$ ) satisfy the inequalities

$$m_{\tilde{\gamma}}, m_{\tilde{z}}, m_{\tilde{w}} < m_{\tilde{l}} < m_{\tilde{q}} < m_{\tilde{g}} \quad (65)$$

where the electroweak gaugino masses are of order 100 GeV, the masses of scalar leptons are of order 200 GeV, and scalar quark masses vary from 350 GeV to 600 GeV.

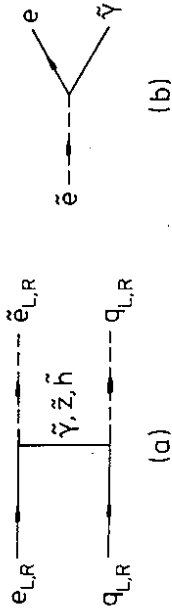


Figure 9. Pair production of scalar electrons and scalar quarks

At HERA the most obvious production process for super-particles is [28] (cf. fig. (9))

$$ep \rightarrow \tilde{e}\tilde{q}X \quad (66)$$

The total cross section falls below 0.05 pb for  $m_{\tilde{e}} + m_{\tilde{q}} > 200$  GeV [29] (cf. fig. (12)). Hence, in view of the present mass bounds for scalar leptons and scalar quarks from LEP and the Tevatron, this process will very likely not be of relevance at HERA.

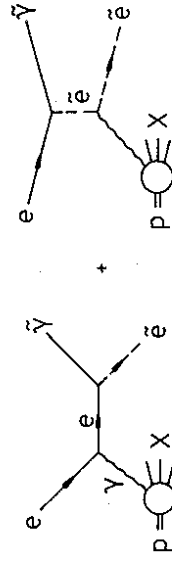


Figure 10. Production of scalar electron and photino

For light photinos a very interesting process is [8] (cf. fig. (10))

$$ep \rightarrow \tilde{e}\tilde{\gamma}X \quad (67)$$

It is a Compton-type process with a bremsstrahlung photon radiated by the proton. This process is of higher order in the coupling than the previous one, but for  $m_{\tilde{\gamma}} = 20 \text{ GeV}$  and  $m_{\tilde{e}} = 60 \text{ GeV}$  the cross section is still about  $0.05 \text{ pb}$  [29]. This process could be seen at HERA although scalar electrons in this mass range are likely to be discovered at LEP II.

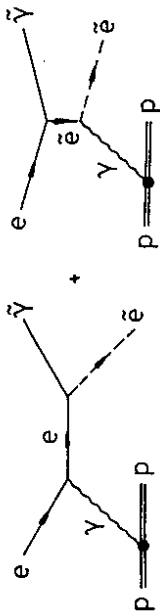


Figure 11. Elastic production of scalar electron and photino

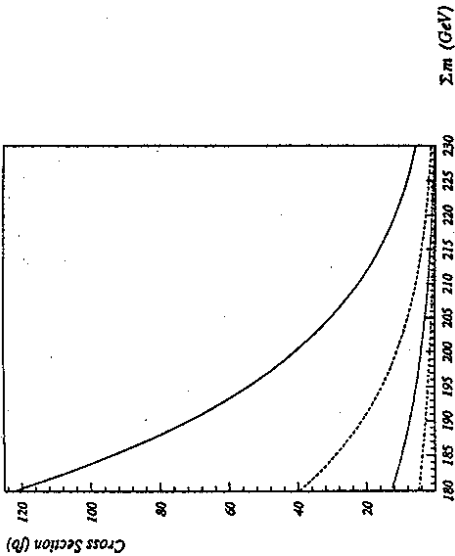


Figure 12. Cross sections for  $ep \rightarrow \tilde{e}_L q_L X$  (full),  $ep \rightarrow \tilde{e}_R q_R X$  (dashed),  $ep \rightarrow \tilde{e}_R q_L X$  (dashed-dotted) at  $\sqrt{s} = 314 \text{ GeV}$  for a typical set of supersymmetry breaking parameters. From [29].

A few years ago, Drees and Zeppenfeld [30] pointed out that the cross section for elastic production of scalar electrons and photinos (cf. fig. (11)) is as large as the inelastic cross section:

$$\sigma(ep \rightarrow \tilde{e}\tilde{\gamma}p) \approx \sigma(ep \rightarrow \tilde{e}\tilde{\gamma}X). \quad (68)$$

The elastic process is interesting, especially since it leads to a very clean final state. The total cross section [31] for the inelastic, the elastic and the quasi-elastic processes are shown in fig. (13).

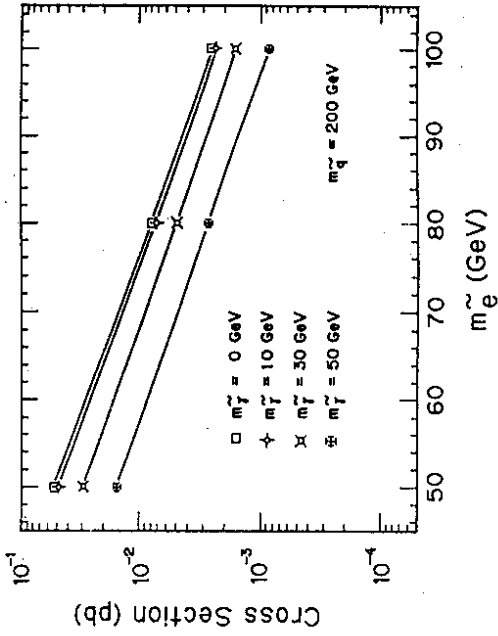


Figure 13. Total cross section for  $ep \rightarrow \tilde{e}\tilde{\gamma}X$ . From [31].

## 5.2 Leptoquarks

The theoretical framework for leptoquarks with Yukawa couplings to quark-lepton pairs are extended gauge theories. It is of interest that such scalar particles with masses of order  $100 \text{ GeV}$  can be consistent with all constraints from rare processes (cf. [32], [33]). However, one should be aware of the fact that for most leptoquarks some fine tuning of couplings is required and that the most general couplings to quark-lepton pairs are usually not compatible with constraints from low energy data. In composite models and technicolour theories leptoquarks usually appear as pseudo-Goldstone bosons which have derivative couplings to fermions pairs.

1. If, by convention, they all carry lepton number +1, their baryon number can be  $+\frac{1}{3}$  or  $-\frac{1}{3}$ . The couplings of all possible leptoquarks to quark-lepton pairs are given in table (3) (cf. [34]). A particularly well studied example is the  $SU(5)$ -type leptoquark  $S_0$  whose couplings to  $SU(2)$ -doublets are:

$$L_I = \lambda_L \bar{q}_L^c i\tau_2 L S_0^\dagger + \text{c.c.} \quad (69)$$

The couplings of scalar leptoquarks are of Yukawa type, and therefore their size may be similar to the size of Higgs boson couplings. In ordinary grand unified theories leptoquark masses are of order  $10^{10}$  GeV or larger. However, in theories where Yukawa couplings violate the unified symmetry, leptoquarks may have masses of order  $m_W$ . In this case baryon- and lepton-number are conserved in the low-energy effective theory.

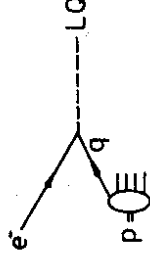


Figure 14. Leptoquark production in electron-quark annihilation

At HERA leptoquarks can be produced as s-channel resonances in the electron-quark subprocess shown in fig. (14). The corresponding Breit-Wigner cross section for a scalar particle reads

$$\sigma_{eq \rightarrow LQ}(s) = \frac{\pi}{s} \frac{\Gamma_{in} \Gamma}{(\sqrt{s} - M)^2 + \Gamma^2/4} \quad (70)$$

$$\rightarrow \frac{4\pi^2}{s} \frac{\Gamma_{in}}{M} \delta(x - \frac{M^2}{s}) \quad (71)$$

It becomes a delta-function in the narrow width approximation. Hence, such narrow resonances appear as peaks in the x-distributions of neutral and charged current cross sections. The electron-proton cross section is given by:

$$\sigma_{ep \rightarrow LQ} = \int_0^1 dx \sigma_{eq \rightarrow LQ}(xs) q(x) \quad (72)$$

$$= \frac{\Gamma_{in}}{M} \sigma_0 \quad (73)$$

$$\sigma_0 = \frac{4\pi^2}{s} q(\frac{M^2}{s}) \quad (74)$$

leptoquark name	left-handed coupling	right-handed coupling	Q	decay channels (coupling)
$S_0$	$\lambda_{L S_0} \bar{q}_L^c i\tau_2 \ell_L S_0^\dagger$	$\lambda_{R S_0} \bar{u}_R^c e_R S_0^\dagger$	$-\frac{1}{3}$	$e_L^+ u$ ( $\lambda_L$ ) $\nu_L d$ ( $-\lambda_L$ ) $e_R^+ u$ ( $\lambda_R$ )
$\tilde{S}_0$		$\lambda_{R \tilde{S}_0} \bar{d}_R^c e_R \tilde{S}_0^\dagger$	$-\frac{1}{3}$	$e_R^+ d$ ( $\lambda_R$ )
$S_1$	$\lambda_{L S_1} \bar{q}_L^c i\tau_2 \vec{\tau} \ell_L S_1^\dagger$		$+\frac{2}{3}$ $-\frac{1}{3}$ $-\frac{1}{3}$ $-\frac{1}{3}$	$\nu_L u$ ( $\sqrt{2}\lambda_L$ ) $\nu_L d$ ( $-\lambda_L$ ) $e_L^+ u$ ( $-\lambda_L$ ) $e_L^+ d$ ( $-\sqrt{2}\lambda_L$ )
$V_{1/2}$	$\lambda_{L V_{1/2}} \bar{d}_R^c \gamma^\mu \ell_L V_{1/2}^\dagger$	$\lambda_{R V_{1/2}} \bar{q}_L^c \gamma^\mu e_R V_{1/2}^\dagger$	$-\frac{1}{3}$ $-\frac{1}{3}$ $-\frac{1}{3}$	$\nu_L d$ ( $\lambda_L$ ) $e_R^+ u$ ( $\lambda_R$ ) $e_L^+ d$ ( $\lambda_L$ ) $e_R^+ d$ ( $\lambda_R$ )
$\tilde{V}_{1/2}$	$\lambda_{L \tilde{V}_{1/2}} \bar{u}_R^c \gamma^\mu \ell_L \tilde{V}_{1/2}^\dagger$		$+\frac{2}{3}$ $-\frac{1}{3}$	$\nu_L u$ ( $\lambda_L$ ) $e_L^+ u$ ( $\lambda_L$ )
$S_{1/2}$	$\lambda_{L S_{1/2}} \bar{u}_R \ell_L S_{1/2}^\dagger$	$\lambda_{R S_{1/2}} \bar{q}_L i\tau_2 e_R S_{1/2}^\dagger$	$-\frac{2}{3}$ $-\frac{1}{3}$ $-\frac{1}{3}$	$\nu_L \bar{u}$ ( $\lambda_L$ ) $e_R^+ d$ ( $-\lambda_R$ ) $e_L^+ \bar{u}$ ( $\lambda_L$ ) $e_R^+ \bar{u}$ ( $\lambda_R$ )
$\tilde{S}_{1/2}$	$\lambda_{L \tilde{S}_{1/2}} \bar{d}_R \ell_L \tilde{S}_{1/2}^\dagger$		$+\frac{1}{3}$ $-\frac{2}{3}$	$\nu_L d$ ( $\lambda_L$ ) $e_L^+ \bar{u}$ ( $\lambda_L$ )
$V_0$	$\lambda_{L V_0} \bar{q}_L \gamma^\mu \ell_L V_0^\dagger$	$\lambda_{R V_0} \bar{d}_R \gamma^\mu e_R V_0^\dagger$	$-\frac{2}{3}$	$\nu_L \bar{u}$ ( $\lambda_L$ ) $e_L^+ d$ ( $\lambda_L$ ) $e_R^+ d$ ( $\lambda_R$ )
$\tilde{V}_0$		$\lambda_{R \tilde{V}_0} \bar{u}_R \gamma^\mu e_R \tilde{V}_0^\dagger$	$-\frac{1}{3}$	$e_R^+ \bar{u}$ ( $\lambda_R$ )
$V_1$	$\lambda_{L V_1} \bar{q}_L \vec{\tau} \gamma^\mu \ell_L V_1^\dagger$		$+\frac{1}{3}$ $-\frac{2}{3}$ $-\frac{1}{3}$ $-\frac{1}{3}$	$\nu_L d$ ( $\sqrt{2}\lambda_L$ ) $\nu_L \bar{u}$ ( $\lambda_L$ ) $e_L^+ d$ ( $-\lambda_L$ ) $e_L^+ \bar{u}$ ( $\sqrt{2}\lambda_L$ )

Table 3. Scalar (S) and vector (V) leptoquarks with the allowed gauge invariant couplings to left- and right-handed fermions. The suffix denotes the weak isospin. From [32].

Leptoquarks with dimensionless couplings to fermions pairs must have spin 0 or spin

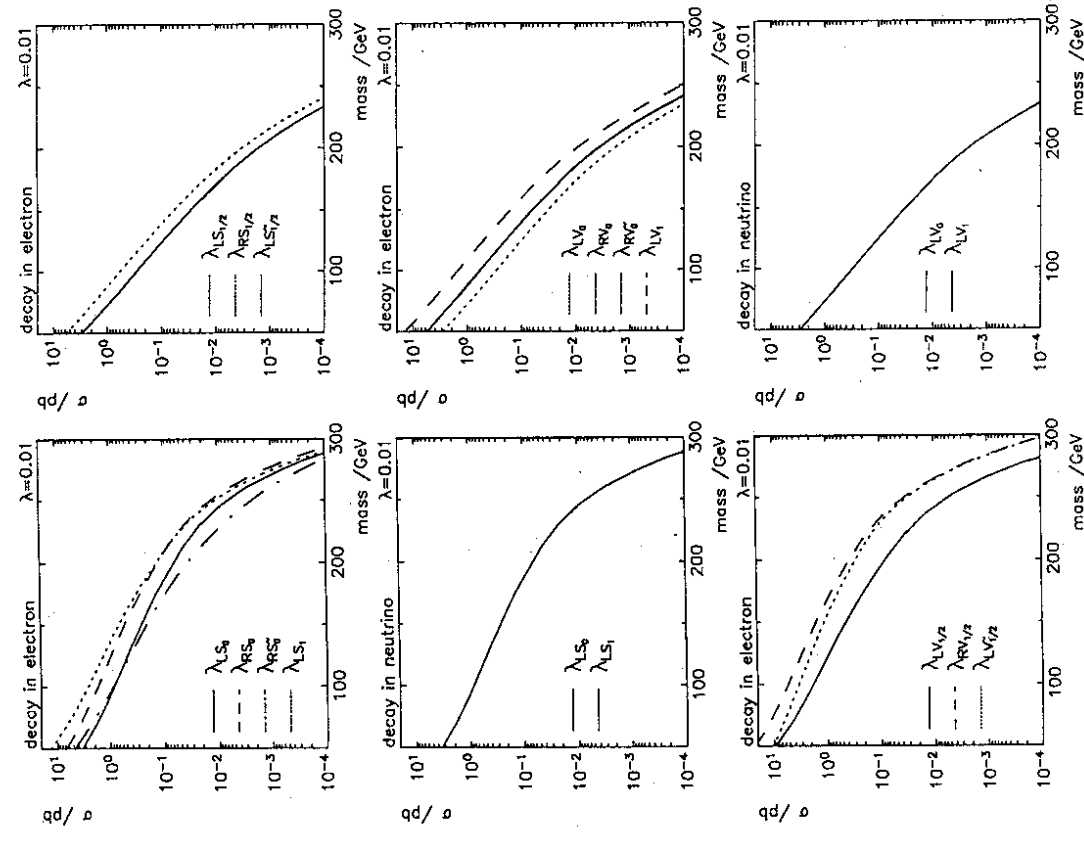


Figure 15.  $2\sigma$ -exclusion limits for leptoquark couplings as functions of leptoquark masses. From [35].

Here  $q(x)$  is the relevant quark distribution inside the proton, and  $\Gamma_{\text{in}} = \lambda^2/16\pi$  is the

partial width for the decay of the leptoquark into the quark-lepton pair in the initial state. For a leptoquark mass  $m_{LQ} \sim 200 \text{ GeV}$  one has  $\sigma_0 = \mathcal{O}(10^4) \text{ pb}$ . Because of this rather large cross section HERA is well suited to search for leptoquarks. For  $\alpha_{LQ} \sim \alpha_{em}$  leptoquarks can be discovered up to the kinematic limit, i.e.,  $m_{LQ} \sim 300 \text{ GeV}$ , and for the small coupling  $\alpha_{LQ} \sim 10^{-3} \alpha_{em}$  one can still find leptoquarks up to  $m_{LQ} \sim 200 \text{ GeV}$ . Discovery limits for all the leptoquarks listed in table (3) are shown in fig. (15). The limits are based on a Monte Carlo study assuming an integrated luminosity of  $100 \text{ pb}^{-1}$  [35]. Mass bounds obtainable for the leptoquark  $\tilde{S}_{1/2}$  from direct search and virtual effects are shown in fig. (16).

First bounds on leptoquark masses have recently been obtained by the collaborations H1 and ZEUS at DESY based on an integrated luminosity of  $25 \text{ nb}^{-1}$ . For left-handed coupling and  $\alpha_{LQ} = \alpha_{em}$  both collaborations find a lower bound of about  $170 \text{ GeV}$  [36],[37].

In supersymmetric models with broken R-parity single production of super-particles is possible. In these models scalar quarks can have direct couplings to electron-quark pairs. Hence, they can be produced in  $ep$ -scattering like leptoquarks and similar bounds on their masses can be expected from HERA experiments [38], [39].

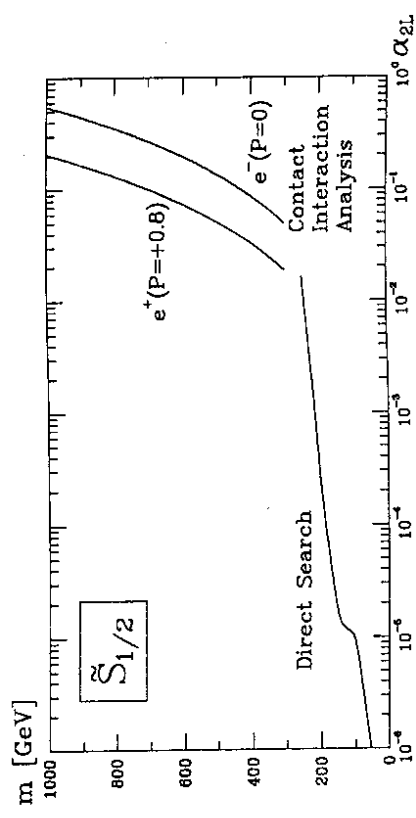


Figure 16. Leptoquark mass bounds from direct search and virtual exchange effects obtainable at HERA as function of the coupling  $\alpha_{2L} = \tilde{h}_{2L}^2/2\pi$ . From [23].

### 5.3 Heavy neutrinos

In extended gauge theories lepton number corresponds to a spontaneously broken, local symmetry. A priori the scale of this symmetry breaking can be anywhere between the Fermi-scale of weak interactions and the grand unification scale  $\Lambda_{GUT} \sim 10^{16} \text{ GeV}$ . A large scale of  $B-L$  breaking implies very small neutrino masses, which may be in the range needed to explain the solar neutrino deficit by means of the MSW-mechanism. In this case we expect no neutral heavy leptons and also no new vector bosons, such as a  $Z'$ , at energies accessible with accelerators.

Alternatively, some theories predict a low scale of  $B-L$  breaking  $\mathcal{O}(1 \text{ TeV})$ . In this case, the ordinary neutrinos are expected to have masses close to the present experimental upper limits. Furthermore, additional vector bosons ( $W_R$  and/or  $Z'$ ) and new heavy neutrinos with masses in the range from a few tens of GeV to a few hundred GeV are predicted. Low energy processes and LEP data require the  $W_R$ -boson to be heavier than 450 GeV [40],[41]. The lower bound increases to 520 GeV, if the lightest right-handed neutrino has a mass below 15 GeV [42]. This leaves an interesting range of  $\nu_R$  and  $W_R$  masses which can be probed for the first time at HERA. In left-right symmetric models with spontaneous parity breaking  $W_R$  bosons have to be heavier than 1-3 TeV [43]. This mass range lies beyond the sensitivity of HERA.

Heavy neutrinos are the simplest example of new heavy leptons and quarks which can be produced via mixing in charged and neutral current processes in  $ep$ -scattering. In the literature new heavy fermions have been discussed in connection with  $E_6$  unified theories, a fourth generation and mirror families [44], [45].

Spontaneous symmetry breaking generates the following mass terms in the neutrino sector:

$$\mathcal{L}_\nu^{\text{mass}} = -\sqrt{L} m_D \nu_R - \frac{1}{2} \bar{\nu}_R^c m \nu_R + \text{h.c.}, \quad (75)$$

$$m_D = g v, \quad m = h v' \quad (76)$$

Here  $g$  and  $h$  are complex  $3 \times 3$  matrices, and the vacuum expectation values  $v'$  and  $v$  break the extended gauge symmetry to  $SU(3)_C \times SU(2)_L \times U(1)_Y$  and to  $SU(3)_C \times U(1)_{em}$ , respectively. The entire mass matrix has to be diagonalized in order to obtain the couplings of  $W$  and  $Z$  bosons to neutrino mass eigenstates. The matrix  $m$  can always be chosen diagonal and real. Assuming  $|\det(m_D)| < \det(m)$ , the weak eigenstates  $\nu_R$  and  $\nu_L$  can be expressed in terms of the Majorana mass eigenstates  $\nu$  and  $N$  as power

series in  $\xi = m_D \frac{1}{m}$  (cf. [46]),

$$\nu_L = \frac{1-\gamma_5}{2} \left( \nu + \xi N - \frac{1}{2} \xi \xi^\dagger \nu + O(\xi^3) \right), \quad (77)$$

$$\nu_R = \frac{1+\gamma_5}{2} \left( N - \xi^\dagger \nu - \frac{1}{2} \xi^\dagger \xi N + O(\xi^3) \right). \quad (78)$$

The corresponding masses of the heavy and light Majorana neutrinos  $N$  and  $\nu$  are given by

$$m_N = m + O\left(\frac{1}{m}\right), \quad (79)$$

$$m_\nu = -m_D \frac{1}{m} m_D^\dagger + O\left(\frac{1}{m^3}\right). \quad (80)$$

The light Majorana neutrinos  $\nu$  are identified with  $\nu_e$ ,  $\nu_\mu$  and  $\nu_\tau$ . Since the Majorana mass matrix  $m$  is large compared to the Dirac mass matrix  $m_D$ , the smallness of the ordinary neutrino masses is naturally explained [47].

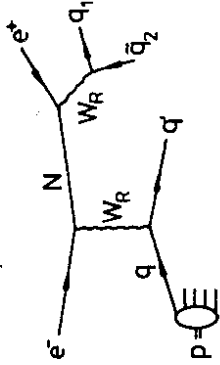


Figure 17. Production and decay of heavy Majorana neutrinos via  $W_R$  exchange

In order to calculate production cross sections for heavy neutrinos one has to express charged and neutral currents in terms of the mass eigenstates. The couplings to the ordinary  $W$ -boson and  $Z$ -boson are given by

$$\mathcal{L}_I = J_{NC}^\mu Z_\mu + J_{CC}^\mu W_\mu^- + J_{CC}^{\mu\dagger} W_\mu^+, \quad (81)$$

where

$$J_{NC}^\mu = \frac{g}{2 \cos \theta_W} \left[ \bar{\nu} \gamma^\mu \frac{1-\gamma_5}{2} \nu + \bar{\nu} \xi \gamma^\mu \frac{1-\gamma_5}{2} N \right. \\ \left. + \bar{N} \xi^\dagger \gamma^\mu \frac{1-\gamma_5}{2} \nu + O(\xi^2) \right], \quad (82)$$

$$J_{CC}^\mu = \frac{g}{\sqrt{2}} \left[ \bar{\nu} V \gamma^\mu \frac{1-\gamma_5}{2} \nu + \bar{\nu} V \xi \gamma^\mu \frac{1-\gamma_5}{2} N + O(\xi^2) \right]. \quad (83)$$



Here  $V$  is a unitary, Kobayashi-Maskawa type mixing matrix in the lepton sector. In addition there are couplings to a heavy  $Z'$ -vector boson and, in the case of left-right symmetric models, are to a heavy charged  $W_R$ -boson.

In  $Z'$ -models the heavy Majorana neutrinos decay predominantly into vector bosons and leptons, i.e.,  $N \rightarrow \ell^\pm W^\mp$  and  $N \rightarrow \nu Z$ . The corresponding partial widths is rather small,

$$\Gamma(N \rightarrow \ell W^\pm) \equiv \Gamma_0 = 26 \text{ MeV} \left( \frac{|\xi_{\nu N}|}{0.1} \right)^2 \left( \frac{m_N}{200 \text{ GeV}} \right)^3 \quad (84)$$

Constraints from low energy experiments on elements of the mixing matrix  $\xi_{ij}$  typically yield  $|\xi| < 0.1$  [48]. In left-right symmetric models the dominant decay proceeds via a virtual  $W_R$  into a charged lepton and three quarks.

The differential cross section for the production of heavy neutrinos via  $W_R$  exchange is easily evaluated. One finds:

$$\frac{d\sigma}{dx dy} = \frac{G_F^2}{2\pi} \frac{m_W^4}{(ys + m_{W_R}^2)^2} \left[ (s - m_N^2) (u(x, \mu^2) + c(x, \mu^2)) + (1-y) (s(1-y) - m_N^2) (\bar{d}(x, \mu^2) + \bar{s}(x, \mu^2)) \right], \quad (85)$$

where  $x$  and  $y$  are restricted to the intervals

$$\frac{m_N^2}{s} \leq x \leq 1, \quad 0 \leq y \leq 1 - \frac{m_N^2}{xs}. \quad (86)$$

Here  $u$ ,  $c$ ,  $d$  and  $s$  denote the densities of up, charm, down and strange quarks in the proton, which depend on the renormalization scale  $\mu$ . The total cross section for the production of heavy neutrinos via mixing is obtained by the replacement  $1/(ys + m_{W_R}^2)^2 \rightarrow |(V\xi)_{eN}|^2 / (ys + m_W^2)^2$  in eq. (85).

The total cross section is obtained from eq. (85) after numerical integration over  $x$  and  $y$ . The result is shown in fig. 18 as function of  $m_N$  for two different  $W_R$  masses and the HERA c.m.s. energy  $\sqrt{s} = 314 \text{ GeV}$ . A rough estimate of the discovery limits for neutrino and  $W_R$  masses with an integrated luminosity of  $200 \text{ pb}^{-1}$  is obtained by requiring 5 events. This yields a maximal neutrino mass of 120 GeV and a maximal vector boson mass of about 700 GeV. The total cross section for the production of heavy Majorana neutrinos via mixing is plotted in fig. 19 for three values of the center of mass energy, corresponding to HERA ( $\sqrt{s} = 314 \text{ GeV}$ ), an upgraded version of HERA ( $\sqrt{s} = 450 \text{ GeV}$ ) and LEP  $\oplus$  LHC ( $\sqrt{s} = 1300 \text{ GeV}$ ). Here  $(V\xi)_{eN} = 0.1$  has been assumed. The discovery limits for the heavy neutrino are 160, 320 and 870 GeV for  $\sqrt{s} = 314, 450, 1300 \text{ GeV}$ , respectively. A detailed Monte Carlo study, including background processes, has been carried out in [49],[50].

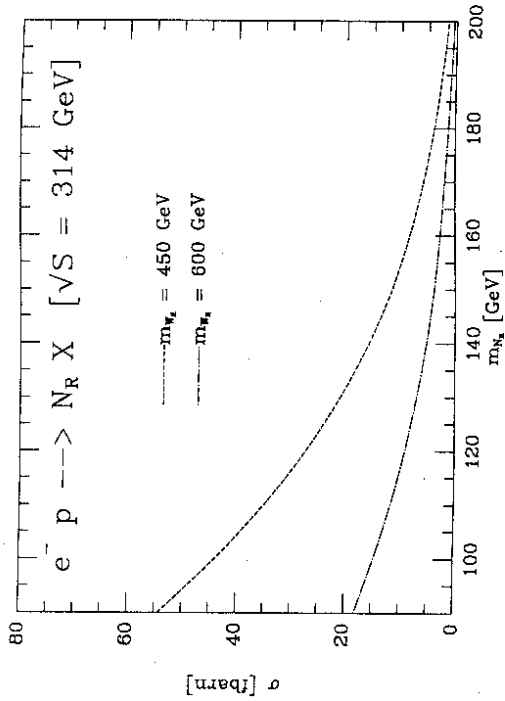


Figure 18. Total cross section for  $ep \rightarrow NX$  via  $W_R$  exchange for two vector boson masses. From [41].

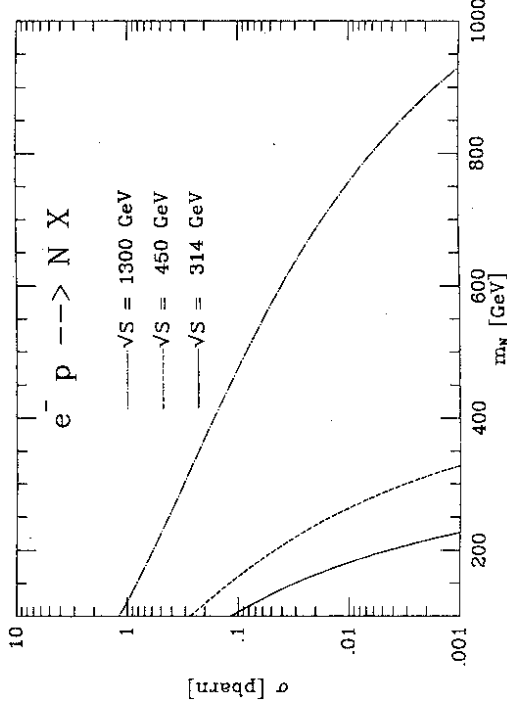


Figure 19. Total cross section for  $ep \rightarrow NX$  via mixing, at three different c.m.s. energies and  $(V\xi)_{eN} = 0.1$ . From [46].

A comprehensive study of other heavy leptons which could be produced at HERA has been carried out in [51]. For charged heavy leptons, which couple to electrons via mixing in the neutral current, the production cross section is slightly smaller than for heavy neutrinos. In composite models heavy states can couple to ordinary leptons and vector bosons via non-renormalizable derivative couplings. For a compositeness scale of 1 TeV one is sensitive to excited electrons and neutrinos with masses up to about 200 GeV and 150 GeV, respectively.

A low scale of  $B - L$  - breaking  $\mathcal{O}(1 \text{ TeV})$  predicts new particles, heavy vector bosons and new heavy leptons, which could be produced at present and future colliders. However, from a cosmological point of view this possibility appears to be disfavoured. The requirement to generate the cosmological baryon asymmetry imposes stringent constraints on the masses of the new states. They have to be much heavier than the  $W$ -boson unless the baryon-asymmetry can be generated at the electroweak phase transition [52].

## 6 Summary

In the previous sections we have discussed what we can hope to learn from electron-proton scattering at HERA about electroweak interactions and about physics beyond the standard model. Among the electroweak processes, i.e., the production of vector bosons and inelastic charged and neutral scattering, the measurement of the strength of the charged current at  $Q^2 \approx 10^4 \text{ GeV}^2$  appears to be most interesting. Within the standard model, after the discovery of the top-quark, one expects to reach an accuracy for the  $W$ -boson mass of

$$\delta m_W = \pm 160 \text{ MeV} \quad (87)$$

This mass, extracted from the  $W$ -propagator, can then be compared with the on-shell mass measured in  $W$ -pair production at LEP1.

A model independent window to new physics are contact interactions. For chirality conserving and chirality changing neutral current contact terms HERA experiments will be sensitive to mass scales up to

$$\Lambda \sim 7 \text{ TeV} \quad (88)$$

A combined analysis of neutral and charged current processes can lead to even more stringent bounds.

In comparison with the Tevatron and LEP2 the search for super-particles is essentially limited to models with broken  $R$ -parity. In this case single production of scalar

quarks is possible, which is very similar to leptoquark production for which HERA is an ideal collider. Even for small couplings rather large leptoquark masses can be probed:

$$\begin{aligned} m_{LQ} &\sim 300 \text{ GeV}, & \alpha_{LQ} &\sim \alpha_{em}, \\ m_{LQ} &\sim 200 \text{ GeV}, & \alpha_{LQ} &\sim 10^{-3} \alpha_{em}. \end{aligned}$$

Also interesting is the single production of charged and neutral heavy leptons. Heavy neutrinos, for instance, could be produced up to a mass of

$$m_N \sim 160 \text{ GeV} \quad (89)$$

The production of heavy leptons in  $ep$ -scattering is the pendant to the production of new heavy vector bosons in  $pp$ -collisions.

## References

- [1] Proc. of the HERA Workshop, Vol.I-II (Hamburg, 1988), ed. R. D. Pececi (in the following referred to as HERA88)
- [2] Physics at HERA, Proc. of the Workshop, Vol.I-III (Hamburg, 1992), eds. W. Buchmüller and G. Ingelman (in the following referred to as HERA92)
- [3] H. Spiesberger, Precision Tests of the Standard Model, preprint BI-TP 93/03 (1993)
- [4] W. Buchmüller, New Particles and Interactions at HERA, in Lepton-Nucleon Interactions at High Energies (World Scientific, Singapore, 1988), ed. F. Barreiro and J. L. Sánchez Gómez, p.259
- [5] F. Schrempp, Searches for New Particles at HERA, preprint DESY 93-096 (1993)
- [6] K. J. F. Gaemers, R. M. Godbole and M. van der Horst, in HERA88, p. 739
- [7] Review of Particle Properties, Phys. Rev. D45, Part 2 (1992)
- [8] G. Alkarelli et al., Nucl. Phys. B262 (1985) 204
- [9] U. Baur, J. A. M. Vermaseren and D. Zeppenfeld, Nucl. Phys. B375 (1992) 3; this paper also contains references to previous work.
- [10] K. Hagiwara et al., Nucl. Phys. B282 (1987) 253
- [11] U. Baur and D. Zeppenfeld, Nucl. Phys. B325 (1989) 253
- [12] T. Helbig and H. Spiesberger, Nucl. Phys. B373 (1992) 73
- [13] S. Godfrey, Z. Phys. C55 (1992) 619
- [14] U. Baur and M. Doncheski, preprint FSU-HEP-920225 (1992)
- [15] M. Böhm and H. Spiesberger, Nucl. Phys. B294 (1987) 1081; *ibid.* B304 (1988) 749
- [16] H. Spiesberger, Nucl. Phys. B349 (1991) 109
- [17] D. Bardin et al., Z. Phys. C42 (1989) 679; *ibid.* C44 (1989) 149
- [18] W. Hollik et al., HERA92, p. 923
- [19] V. Brisson et al., HERA92, p. 947
- [20] W. Buchmüller and D. Wyler, Nucl. Phys. B268 (1986) 621
- [21] R. Rückl, Phys. Lett. 129B (1983) 363; Nucl. Phys. B234 (1984) 91
- [22] W. Buchmüller, B. Lampe and N. Vlachos, Phys. Lett. 197B (1987) 379
- [23] P. Haberl, F. Schrempp and H.-U. Martyn, HERA92, p. 1133; this paper also contains references to previous work
- [24] P. Haberl et al., HERA92, p. 980; H.-U. Martyn et al., HERA92, p. 987; these papers also contain references to previous work
- [25] M. A. Doncheski and J. L. Hewett, Z. Phys. C56 (1992) 209
- [26] J. Ellis, S. Kelley and D. V. Nanopoulos, Phys. Lett. B249 (1990) 441; U. Amaldi, W. de Boer and H. Fürstenau, Phys. Lett. B260 (1991) 447; P. Langacker and M. Luo, Phys. Rev. D44 (1991) 817; P. Langacker and N. Polonsky, Phys. Rev. D47 (1993) 4028
- [27] G. G. Ross and R. G. Roberts, Nucl. Phys. B377 (1992) 571; R. Arnowitt and P. Nath, Phys. Rev. Lett. 69 (1992) 725; S. Kelley et al., Nucl. Phys. B398 (1993) 3
- [28] S. K. Jones and C. H. Llewellyn Smith, Nucl. Phys. B217 (1983) 145
- [29] A. Bartl et al., HERA92, p. 1118
- [30] M. Drees and D. Zeppenfeld, Phys. Rev. D39 (1989) 2536
- [31] H. Tsutsui et al., Phys. Lett. 245B (1990) 663
- [32] B. Schrempp, HERA92, p. 1034
- [33] P. Langacker, M.-X. Luo and A. K. Mann, Rev. Mod. Phys. 64 (1992) 87
- [34] W. Buchmüller, R. Rückl and D. Wyler, Phys. Lett. B191 (1987) 442
- [35] P. Schleper, HERA92, p. 1043
- [36] ZEUS collaboration, M. Derrick et al., Phys. Lett. B306 (1993) 173
- [37] H1 collaboration, I. Abt et al., Nucl. Phys. B396 (1993) 3

- [38] J. Butterworth and H. Dreiner, *HERA92*, p. 1079
- [39] T. Kon, T. Kobayashi and K. Nakamura, *HERA92*, p.1088
- [40] J. Polak and M. Zralek, *Nucl. Phys. B363* (1991) 385; *Phys. Lett. B276* (1992) 492
- [41] W. Buchmüller and C. Greub, *Nucl. Phys. B381* (1992) 109
- [42] F. Abe et al., *Phys. Rev. Lett.* 67 (1991) 2609
- [43] G. Beall, M. Bender and A. Soni, *Phys. Rev. Lett.* 48 (1982) 848;  
G. Ecker and W. Grimus, *Nucl. Phys. B258* (1985) 328
- [44] F. M. L. Almeida Jr., J. A. Martins Simões, A. J. Ramalho, *Nucl. Phys. B347* (1990) 537
- [45] F. Csikor and I. Montvay, *Phys. Lett.* 231B (1989) 503;  
F. Csikor, *Z. Phys.* C49 (1991) 129
- [46] W. Buchmüller and C. Greub, *Nucl. Phys. B363* (1991) 345
- [47] T. Yanagida, in *Workshop on Unified Theories*, KEK report 79-18 (1979) p.95;  
M. Gell-Mann et al., in *Supergravity*, eds. P. van Nieuwenhuizen and D. Freedman  
(North Holland, Amsterdam 1979) p. 315
- [48] P. Langacker and D. London, *Phys. Rev. D38* (1988) 907;  
W. Buchmüller, C. Greub and H.-G. Kohrs, *Nucl. Phys. B370* (1992) 3;  
E. Nardi, E. Roulet and D. Tommasini, *Phys. Rev. D46* (1992) 3040
- [49] F. Kole et al., *HERA92*, p. 1003
- [50] G. Ingelman and J. Rathsmann, preprint DESY 93-039
- [51] F. Boudjema et al., *HERA92*, p. 1094
- [52] K. Enqvist and I. Vija, *Phys. Lett. B299* (1993) 281;  
W. Buchmüller and T. Yanagida, *Phys. Lett. B302* (1993) 240